International Journal of Science and Engineering Applications
Volume 14-Issue 11, 109 – 113, 2025, ISSN:- 2319 - 7560
DOI: 10.7753/IJSEA1411.1019

Wind-Solar-Energy Storage DC Microgrid: Design of Droop Coordination Strategy and Dual Closed-Loop Control and Simulation

Yin Liu [1] Ran Chen [1] Jinmao Li [1]
[1] School of Electronic Information and Electrical Engineering, Yangtze University, Jingzhou, China

Abstract: With the rapid development of new energy power generation and the widespread application of DC microgrids, this paper tackles power coordination and smooth grid-connected/off-grid switching issues in multi-distributed power source parallel operation. A wind-photovoltaic-storage integrated DC microgrid simulation model is constructed, adopting droop control as the core coordination strategy and a dual closed-loop control (voltage outer loop + current inner loop) for the battery energy storage module. The model includes a permanent magnet direct-drive (PMDD) wind power system, a photovoltaic system with incremental conductance MPPT, and an energy storage system for power balance. Simulations on MATLAB/Simulink (initial irradiance 1000W/m², wind speed 4.8m/s; 1s disturbance: 800W/m², 5.2m/s) show: DC bus voltage stabilizes near 900V with ±2% fluctuation (within ±5% allowable range); wind/photovoltaic units achieve stable output in 0.1s; energy storage fluctuates ±1%, enhancing anti-disturbance. This research resolves parallel power conflicts, supports grid switching, and lays a foundation for practical engineering.
Keywords: DC microgrid; MPPT; Wind power generation; Droop control

1. Introduction

Against the backdrop of the vigorous development of global new energy power generation technologies and the increasingly widespread application of DC microgrids, this paper specifically designs a grid-connected/off-grid switching simulation model based on wind-photovoltaic-storage droop control to address the issues of power coordination and smooth grid-connected/off-grid switching during the parallel operation of multiple distributed power sources[1]. The model takes wind power generation module, photovoltaic power generation module and battery energy storage module as the core components. Among them, the wind power generation module is responsible for capturing wind energy and converting it into electrical energy.[2] The photovoltaic power generation module converts solar energy into usable electricity through the photovoltaic effect, and the battery energy storage module undertakes key functions such as energy storage, fluctuation suppression and emergency power supply. The three work synergistically to form a stable distributed energy supply system. To achieve efficient operation in the scenario of multiple parallel power sources, the droop control strategy is intentionally introduced into the model. By simulating the droop characteristics of power output, it dynamically adjusts the output power distribution ratio of each distributed power source, ensuring that the DC bus voltage is always maintained within a stable range. This effectively avoids power conflicts and mutual interference that may occur when multiple power sources are connected in parallel and provides reliable technical support for the smooth switching of the system between grid-connected and off-grid operation modes.

First, this paper systematically establishes a comprehensive structural framework for the DC microgrid, which is centered on the core objectives of efficient utilization of distributed energy and stable operation of the system, encompassing four key components. Among them, the power generation module takes renewable energy sources such as wind energy and solar energy as the core, responsible for converting natural energy into DC electrical energy to provide basic power supply for the system; the energy storage module adopts battery energy storage units, mainly undertaking the tasks of electrical energy storage, power fluctuation suppression, and addressing energy supply gaps to ensure the system's energy balance; the grid-connection module serves as a key interface connecting the system to the external main grid, realizing bidirectional power transmission and switching control between grid-connected and off-grid modes to ensure the coordinated operation of the system and the grid; the droop control design is embedded in the framework as a core control strategy, providing technical support for the coordinated power distribution under the scenario of multiple parallel power sources by dynamically adjusting the output characteristics of each power source.

To verify the feasibility and stability of the designed structural framework, this paper finally selects the MATLAB/Simulink simulation platform to establish a complete simulation experimental model. During the simulation process, by reasonably configuring the core parameters of each module, the energy supply fluctuation scenarios under different illumination and wind speed conditions, as well as the typical operating conditions of grid-connected/off-grid mode switching, are simulated, and the variation law of the DC bus voltage is analyzed. The simulation results show that the established simulation model can effectively resist the impacts caused by the output fluctuations of distributed energy sources and always maintain the DC bus voltage within the preset reasonable range. This fully verifies the effectiveness of the structural framework design and the droop control strategy, providing a reliable simulation basis for the development and optimization of subsequent practical systems.

International Journal of Science and Engineering Applications
Volume 14-Issue 11, 109 – 113, 2025, ISSN:- 2319 - 7560
DOI: 10.7753/IJSEA1411.1019

2. DC Microgrid System Structure

To achieve efficient adaptation and coordinated operation between each distributed unit and the DC bus, all power generation units and energy storage units in the system must be connected to the DC bus through dedicated power electronic converters [3]. Specifically, DC/DC converters are mainly responsible for regulating the output voltage levels of different units to align with the preset voltage standard of the DC bus, thereby eliminating transmission barriers caused by voltage differences and ensuring stable power transmission. In contrast, DC/AC converters realize bidirectional conversion between DC power and AC power to meet the requirements of certain AC-output power consumption scenarios or energy interaction between the system and the external AC grid, which effectively expands the system's application scope and interactive compatibility [4]. For the DC microgrid system studied in this paper, its detailed topological structure and the connection relationships among various components are shown in Figure 1 below.

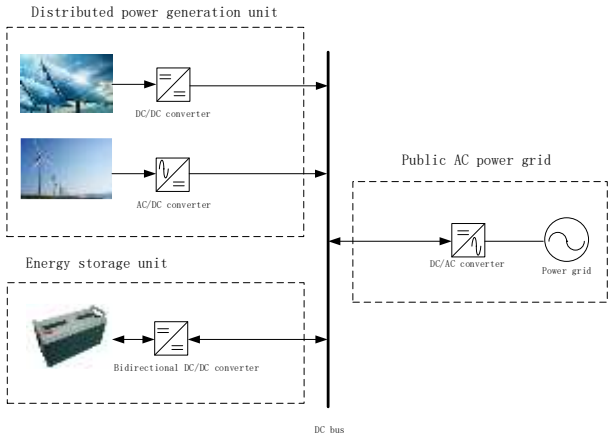

Figure 1: Topological Structure Diagram of the DC Microgrid

3. Design of the Power Generation Module

3.1 Wind Power Generation Module

The wind power generation part adopts a permanent magnet direct-drive (PMDD) wind power generation system, and its equivalent circuit diagram is shown in Figure 2. First, the wind turbine captures wind energy from nature and efficiently converts wind energy into mechanical energy through blade rotation and mechanical transmission mechanisms. Subsequently, the permanent magnet synchronous generator (PMSG) receives this mechanical energy and initiates the electromagnetic induction process, completing the stable conversion from mechanical energy to electrical energy and producing initial electrical energy suitable for subsequent transmission [5]. Finally, the transformer adjusts the voltage of the electrical energy in accordance with the voltage level standards of the power grid. After the electrical energy parameters meet the grid-connection requirements, the electrical energy is smoothly fed into the public power grid to achieve power absorption.

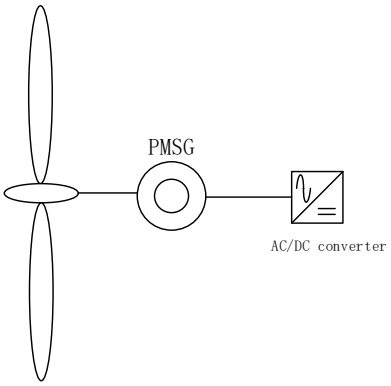

Figure 2: Equivalent Circuit of the Permanent Magnet Direct-Drive (PMDD) Wind Power Generation System

The formulas for the wind turbine are as follows:

$$P_W = 0.5\rho A v^3 C_p$$

$$\gamma = \frac{\omega_r}{v}$$

P_W denotes the wind turbine output power, A represents the swept area of the wind turbine blades, ρ is the air density, v stands for the wind speed and C_p refers to the wind energy utilization coefficient. The calculation formula for C_p is as follows:

$$C_p = c_1\left(\frac{c_2}{\lambda_1} - c_3\theta - c_4\right)e^{\left(\frac{-c_5}{\lambda_1}\right)} + c_6\lambda$$

θ is the pitch angle, c_1 to c_6 take the values of 0.5158、118、0.5、5、24、0.0068.

3.2 Photovoltaic Power Generation Module

The photovoltaic power generation control employs the incremental conductance method, and its derivation process is as follows:

$$\frac{dP}{dV} = \frac{d(V \cdot I)}{dV} = I + V \cdot \frac{dI}{dV}$$

At the maximum power point (MPP), the derivative of power with respect to voltage, $\frac{dP}{dV}$, should be equal to zero:

$$I + V \cdot \frac{dI}{dV} = 0$$

Here, $\frac{dI}{dV}$ denotes the derivative of current I with respect to voltage V, which is usually approximated using conductance G and incremental conductance ΔG.

International Journal of Science and Engineering Applications
Volume 14-Issue 11, 109 – 113, 2025, ISSN:- 2319 - 7560
DOI: 10.7753/IJSEA1411.1019

$$G = \frac{dI}{dV}$$

When $G > -\frac{I}{V}$, the voltage is adjusted upward; when $G < -\frac{I}{V}$, the voltage is adjusted downward; and when $G = -\frac{I}{V}$, the system has reached the maximum power point (MPP). The working principle of the circuit is as follows: a reference voltage V_{ref} is generated by the MPPT algorithm, and this V_{ref} is compared with the real-time voltage collected by the controller. The resulting error signal is transmitted to the proportional-integral (PI) controller, which outputs the duty cycle d. Finally, a PWM (Pulse-Width Modulation) signal is generated to control the DC/DC converter. The block diagram of the circuit is shown in Figure 3.

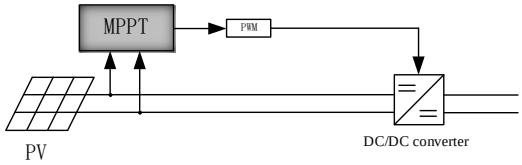

Figure 3: Block Diagram of the Photovoltaic (PV) Module

4.Energy Storage and Grid-Connected Module

4.1Design of the Energy Storage Module

The energy storage system not only stabilizes the DC bus but also functions to balance power. To achieve power balance, a dual closed-loop control strategy is adopted, consisting of an outer voltage loop and an inner current loop. The outer voltage loop stabilizes the DC bus voltage, while the inner current loop controls the charging/discharging current to track the reference value

4.2 Droop Control Design

The core idea of droop control is to establish a linear droop relationship between the output voltage and output power of power sources, thereby achieving autonomous power distribution when multiple power sources operate in parallel [6]. When changes in system load cause fluctuations in the DC bus voltage, each power source automatically adjusts its output power according to its own droop characteristics [7]. This not only ensures that the bus voltage is maintained within the allowable range but also distributes the load power in a preset proportion, avoiding mutual interference between power sources. For distributed power sources in DC microgrids, the basic mathematical model of droop control is as follows:

$$U_{ref,i} = U_0 - k_{P,i} \cdot P_i$$

A dual closed-loop control strategy with a voltage outer loop and a current inner loop is adopted. The voltage outer loop stabilizes the DC bus voltage, while the current inner loop controls the charging/discharging current to follow the reference value. The difference between the voltage reference value U_{dcref} and the actual value U_{dc} is processed by the PI regulator to generate the current reference value I^*_{gd}. Subsequently, the difference between the current reference value I^*_{gd} and the actual charging/discharging current value I_{gd} is processed by the PI regulator to generate the target duty cycle. The duty cycle voltage U^*_{gd} is compared with the triangular carrier voltage value ΔU_{gd} to generate two complementary PWM signals, which are then sent to the gate of the switching device in the bidirectional DC/DC converter. The block diagram of this control structure is shown in Figure 4.

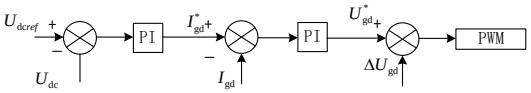

Figure 4: Control Diagram of the Energy Storage Module

In the formula $U_{ref,i}$ is the output voltage reference value of the *i-th* power source, U_0 is the rated no-load output voltage of all power sources, $K_{P,i}$ is the active power droop coefficient of the *i-th* power source, P_i is the actual output active power of the i-th power source. It can be seen from the mathematical model that the output voltage of the power source decreases linearly with the increase of output power. By adjusting the droop coefficient $K_{P,i}$, the regulation of the power distribution ratio among different power sources can be achieved.

In the formula $U_{ref,i}$ is the output voltage reference value of the *i-th* power source, U_0 is the rated no-load output voltage of all power sources, $K_{P,i}$ is the active power droop coefficient of the *i-th* power source, P_i is the actual output active power of the i-th power source. It can be seen from the mathematical model that the output voltage of the power source decreases linearly with the increase of output power. By adjusting the droop coefficient $K_{P,i}$, the regulation of the power distribution ratio among different power sources can be achieved.

5. Simulation and Results

Based on the above design methods, a simulation model was built using MATLAB/Simulink. The DC bus voltage reference value is set to 900V, the initial irradiance is 1000W/m², and the initial wind speed is 4.8m/s. At 1s, the irradiance suddenly changes to 800W/m², and the wind speed suddenly changes to 5.2m/s. The simulation results of each unit are shown in Figure 5.

International Journal of Science and Engineering Applications
Volume 14-Issue 11, 109 – 113, 2025, ISSN:- 2319 - 7560
DOI: 10.7753/IJSEA1411.1019

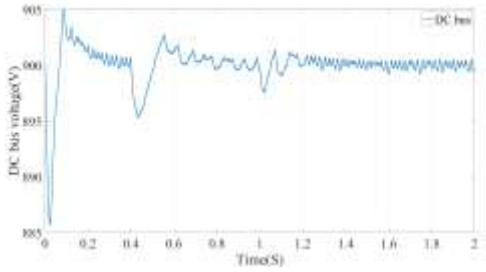

(a)DC bus voltage

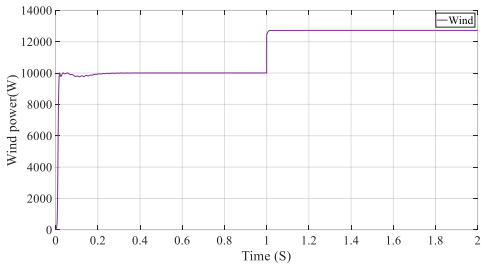

(b)Wind power

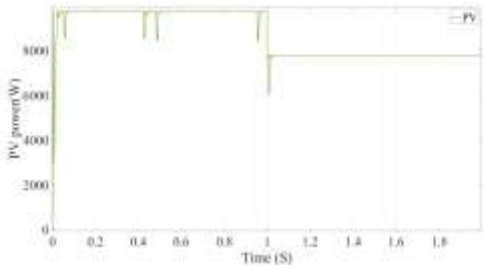

(c)PV power

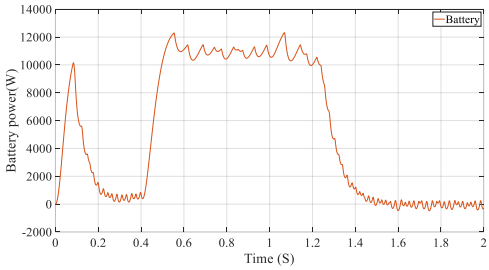

(d)Battery power

Figure 5. Voltage and power of each module

As can be clearly observed from the DC bus voltage simulation waveform shown in Figure 5(a), during the initial stage of system start-up (0~0.5s), there is a small dynamic fluctuation in the bus voltage due to the coordinated start-up transition process of distributed power sources (photovoltaic and wind turbine) and energy storage units. After 0.5s, however, the voltage quickly converges and stabilizes near the rated reference value of 900V, with only slight oscillations within ±2%. This fluctuation range is fully within the system's preset allowable range of ±5%, which fully verifies the accurate voltage regulation effect of the voltage outer loop control on the DC bus voltage, as well as the effectiveness of the dual closed-loop control strategy in suppressing voltage oscillations and improving the steady-state performance of the system.

Analysis of the wind turbine output power waveform in Figure 5(b) and the photovoltaic output power waveform in Figure 5(c) shows that under the operating condition disturbance set in the simulation—where irradiance suddenly changes from 1000W/m² to 800W/m² and wind speed suddenly changes from 4.8m/s to 5.2m/s at 1s—the wind turbine and photovoltaic units quickly respond to changes in external environmental parameters through the synergistic effect of their own MPPT control strategies and the system's droop control. After a short dynamic adjustment period (approximately 0.1s transition time), stable power output is achieved after 1s. From the waveform characteristics, there is no obvious overshoot or oscillation in power output: the wind turbine output power stabilizes near the maximum wind energy capture value corresponding to the wind speed, and the photovoltaic output power is consistent with the irradiance change trend and remains smooth. This indicates that both the power tracking capability of the distributed power generation units and the dynamic response characteristics of the system meet the design expectations.

Looking further at the output power waveform of the battery energy storage unit shown in Figure 5(d), it can be found that the battery starts to enter the power output stage at 0.4s and maintains a stable power output state until 1.2s, with the power fluctuation range controlled within ±1%. This result shows that the current inner loop control of the bidirectional DC/DC converter effectively achieves accurate tracking of the charging/discharging current to the reference value. As a result, the battery can provide temporary support for the stability of the bus voltage during the initial stage of system start-up (0.4~1s), and at the same time play an energy storage buffering role during the transition period of the operating condition mutation at 1s. Through smooth power output, it suppresses the impact of sudden power changes of distributed power sources on the system, further verifying the rationality of the cooperation between the dual closed-loop control and droop control, as well as the core role of the energy storage unit in improving the system's anti-disturbance capability and ensuring power balance.

6. Conclusion

This paper addresses the power coordination and smooth grid-connected/off-grid switching issues in wind-solar-energy storage DC microgrids by designing an integrated system with wind, photovoltaic, and battery energy storage modules, adopting droop control as the core coordination strategy and dual closed-loop control for the energy storage module. MATLAB/Simulink simulation results confirm the design's effectiveness: the DC bus voltage stabilizes near 900V with ±2% fluctuations (within the ±5% allowable range) after start-up; wind and photovoltaic units achieve stable power output

within 0.1s under environmental disturbances via MPPT and droop control synergy; the battery energy storage unit maintains power balance with ±1% fluctuation, enhancing system anti-disturbance capability. This research resolves parallel power conflicts and voltage instability, providing technical support for grid-connected/off-grid switching. Future work may involve optimizing droop coefficients with intelligent algorithms, expanding extreme working condition simulations, and verifying via hardware-in-the-loop experiments.

7. References

[1] H. Li, Y. Wang, and Z. Zhang, "Design and Simulation of Wind-Solar-Battery Hybrid Microgrid System with MPPT Control," IEEE Access, vol. 11, pp. 45218-45229, 2023, doi: 10.1109/ACCESS.2023.3276541.

[2] M. A. Khan, A. Ali, and S. Kim, "Comprehensive Review of Wind-Solar-Battery Hybrid Microgrids: Configuration, Control, and Optimization," Renewable and Sustainable Energy Reviews, vol. 167, 112789, 2022, doi: 10.1016/j.rser.2022.112789.

[3] H. Zhang, X. Wang, Y. Li, and Z. Chen, "Interface Converters for Distributed Energy Storage in DC Microgrids: Topologies, Control, and Applications," *IEEE Journal of Emerging and Selected Topics in Power Electronics*, vol. 9, no. 5, pp. 5686-5702, 2021, doi: 10.1109/JESTPE.2020.3045124.

[4] Farag A Y, Biadene D, Caldognetto T, et al. Enhancing DC microgrids integration with three-phase AC grids using multiport converters[C]/IET Conference Proceedings CP878. Stevenage, UK: The Institution of Engineering and Technology, 2024, 2024(3): 234-239.

[5] Aouichak I, Jacques S, Bissey S, et al. A bidirectional grid-connected DC – AC converter for autonomous and intelligent electricity storage in the residential sector[J]. Energies, 2022, 15(3): 1194.

[6] Zhifu W, Yupu W, Yinan R. Design of closed-loop control system for a bidirectional full bridge DC/DC converter[J]. Applied energy, 2017, 194: 617-625.

[7] Khaledian A, Golkar M A. Analysis of droop control method in an autonomous microgrid[J]. Journal of applied research and technology, 2017, 15(4): 371-377